# HLA-B-associated transcript 3 (Bat3/Scythe) negatively regulates Smad phosphorylation in BMP signaling

K Goto[1], KI Tong[1], J Ikura[1] and H Okada*[1,2]

Members of the transforming growth factor-$\beta$ (TGF-$\beta$) superfamily participate in numerous biological phenomena in multiple tissues, including in cell proliferation, differentiation, and migration. TGF-$\beta$ superfamily proteins therefore have prominent roles in wound healing, fibrosis, bone formation, and carcinogenesis. However, the molecular mechanisms regulating these signaling pathways are not fully understood. Here, we describe the regulation of bone morphogenic protein (BMP) signaling by Bat3 (also known as Scythe or BAG6). Bat3 overexpression in murine cell lines suppresses the activity of the *Id1* promoter normally induced by BMP signaling. Conversely, Bat3 inactivation enhances the induction of direct BMP target genes, such as *Id1*, *Smad6*, and *Smad7*. Consequently, Bat3 deficiency accelerates the differentiation of primary osteoblasts into bone, with a concomitant increase in the bone differentiation markers *Runx2*, *Osterix*, and *alkaline phosphatase*. Using biochemical and cell biological analyses, we show that Bat3 inactivation sustains the C-terminal phosphorylation and nuclear localization of Smad1, 5, and 8 (Smad1/5/8), thereby enhancing biological responses to BMP treatment. At the mechanistic level, we show that Bat3 interacts with the nuclear phosphatase small C-terminal domain phosphatase (SCP) 2, which terminates BMP signaling by dephosphorylating Smad1/5/8. Notably, Bat3 enhances SCP2–Smad1 interaction only when the BMP signaling pathway is activated. Our results demonstrate that Bat3 is an important regulator of BMP signaling that functions by modulating SCP2–Smad interaction.
*Cell Death and Disease* (2011) **2**, e236; doi:10.1038/cddis.2011.114; published online 1 December 2011
**Subject Category:** Cancer

Members of the transforming growth factor-$\beta$ (TGF-$\beta$) super-family control a plethora of cellular responses, including cell proliferation, stem cell renewal, differentiation, extracellular matrix remodeling, and embryonic development.[1–3] TGF-$\beta$ superfamily proteins include the TGF-$\beta$s, activins, and bone morphogenic proteins (BMPs). These molecules are ligands that engage a complex composed of type I receptor and type II receptors to initiate intracellular signaling. This ligand-dependent formation of the active receptor complex leads to the phosphorylation of type I receptor by type II receptor. Activated type I receptors in turn recruit specific receptor-activated Smads (R-Smads), depending on the ligand. Smad1, 5, and 8 (Smad1/5/8) are recruited in response to BMP binding, whereas Smad2 and 3 are recruited in response to TGF-$\beta$s and activins. Activated type I receptor then phosphorylates a Ser–Ser–X–Ser (SSXS) motif in the C-terminal region of the R-Smads, activating them. Activated R-Smads in turn form hetero-oligomeric complexes with the common mediator Smad4 (the Co-Smad), translocate to the nucleus, and regulate transcription of their target genes. Structurally, R-Smads contain Mad homology 1 (MH1) and Mad homology 2 (MH2) domains, which are connected by a linker region. The Co-Smad also contains the MH1, linker, and MH2 domains but lacks the SSXS motif.

The ongoing discovery of an increasing number of Smad phosphatases suggests that dephosphorylation is a critical mechanism for terminating Smad activity. Protein phosphatase 1A, magnesium-dependent, $\alpha$-isoform (PPM1A) mediates the C-terminal dephosphorylation of Smad2/3[4] and Smad1.[5] Additional Smad1 phosphatases include pyruvate dehydrogenase phosphatase 1 and 2, and the small C-terminal domain phosphatase (SCP) 1 and 2.[6,7] Dephosphorylation of Smad1 by any one of these phosphatases attenuates BMP signaling. In contrast, SCPs can enhance the transcriptional activity of Smad2/3 by removing an inhibitory phosphate moiety in the linker region.[8] However, relatively little is known about the signaling pathways that regulate Smad dephosphorylation.

*Bat3* (also called *Scythe*[9] or *BAG6*) was originally identified as a gene located within the class III region of the human major histocompatibility complex on chromosome 6.[10] Bat3 has been reported to regulate NK cell signaling,[11] histone methylation,[12] and apoptosis in a variety of settings,[9,13–17] suggesting that Bat3 is a mediator in diverse signaling

pathways. Recent reports suggest that it has critical roles in targeting of tail-anchored proteins to the endoplasmic reticulum[18,19] and in degradation of mislocalized and misfolded proteins.[20,21] Relevant to our current study, Bat3 was reported to interact with TGF-$\beta$ receptors and to enhance TGF-$\beta$-induced expression of type I collagen (ColIA).[22] Although nuclear Bat3 appeared to be critical for this event, the underlying molecular mechanism remains unclear.

In this study, we present evidence implicating Bat3 as a negative regulator of BMP signaling. RNAi-mediated depletion of Bat3 sustains BMP target gene induction and enhances BMP-mediated osteoblast differentiation. In the absence of Bat3, C-terminal phosphorylation of Smad1/5/8 is markedly prolonged. At the protein level, Bat3 physically interacts with a nuclear phosphatase, SCP2, that regulates Smad1/5/8 phosphorylation. In the presence of Bat3, the interaction of SCP2 with Smad1 that is triggered by activation of BMP signaling is increased. On the basis of our data, we propose a model in which Bat3 regulates BMP signaling pathways by modulating SCP2-mediated dephosphorylation of Smads.

## Results

**Bat3 is a suppressor of BMP signaling.** Bat3 overexpression in murine mesangial cells was reported to induce TGF-$\beta$ target genes, including ColIA.[22] However, the molecular mechanism by which Bat3 regulates TGF-$\beta$ signaling is a mystery. Neither is it known whether Bat3 can regulate the functions of other TGF-$\beta$ superfamily members such as BMP. To address these questions, we first used a reporter system to examine whether Bat3 can influence the transactivation activity of *Id1*, an immediate-early BMP target gene.[23] We co-transfected U2OS human osteosarcoma cell line with separate constructs expressing Bat3–Myc, an *Id1*–luciferase (*luc*) reporter gene, and an HA-tagged, constitutively active (QD) form of a BMP receptor (activin receptor-like kinase (ALK) 2-, ALK3- or ALK6-QD[24]). We found that, rather than enhancing BMP target gene expression, Bat3 overexpression greatly suppressed the Id1 promoter activity induced by all ALKs-QD (Figure 1a). These data suggest that Bat3 negatively, rather than positively, regulates BMP signaling.

To test whether Bat3 had a negative impact on BMP signaling in a biological setting, we transfected C2C12 mouse myoblast cells with small interfering RNA (siRNA) oligo duplexes specific for mouse Bat3 (siBat3) or a control scrambled siRNA (siControl; siCNT; Supplementary Figure 1A). We cultured these cells with 100 ng/ml BMP-2 for 3, 24, or 48 h and examined mRNA levels of the BMP target genes *Id1*, *Smad6*, and *Smad7*. Transcript levels of all these target genes were comparable between control and Bat3-depleted cells after 3 h of BMP treatment (Figure 1b). However, higher levels of all target gene mRNAs were observed in Bat3-depleted cells compared with control cells after 24 h BMP treatment. This sustained induction of BMP target genes in Bat3-depleted cells was even more prominent after 48 h, whereas transcript levels of all target genes in siCNT cells after 48 h in BMP were comparable to those in untreated cells (Figure 1b). Similar results were obtained when primary osteoblasts were isolated from wild-type (WT) or gene-targeted Bat3-deficient

($Bat3^{-/-}$) mice[17] and treated with BMP-2 for 3 or 48 h. Enhanced induction of the same BMP target genes was observed in extracts of BMP-treated $Bat3^{-/-}$ osteoblasts at 48 h compared with BMP-treated WT controls (Figure 1c). These data further support our initial observation that Bat3 negatively regulates the induction of BMP target genes.

**Bat3 inactivation sustains C-terminal phosphorylation of Smad1/5/8.** Although a previous report had indicated that nuclear Bat3 could enhance TGF-$\beta$ signaling,[22] our data above suggested the opposite conclusion. We speculated that Bat3 might have an indirect modulatory effect on the function of nuclear components of BMP signaling. Phosphorylation is a key means of regulating Smad functions.[25] To determine the role of Bat3 in Smad phosphorylation, we transfected C2C12 cells with lentivirus expressing shRNA against Bat3 (shBat3) or control shRNA (shCNT; Supplementary Figure 1B) and treated these cells with 50 ng/ml BMP-2 for 0, 1, 12, 24, or 36 h. Levels of phosphorylated Smad1/5/8 in cell extracts were determined using an antibody (Ab) specific for the phosphorylated C-terminal region of Smad1/5/8 (pSmad1/5/8-CT). We found that pSmad1/5/8-CT levels were significantly higher and sustained over time in cells depleted of Bat3 (Figure 2a).

To confirm this finding in intact cells, we cultured C2C12 shCNT and shBat3 cells with 100 ng/ml BMP-2 for 0; 1; 12; or 24 h, fixed the cells, and stained them with anti-pSmad1/5/8-CT Ab (Figure 2b). Before BMP treatment, only trace amounts of pSmad1/5/8-CT were present in the cytosol of both shCNT and shBat3 cells. After 1 h of BMP treatment, pSmad1/5/8-CT levels were markedly increased but appeared equal in the nuclei of shCNT and shBat3 cells. However, after 12 h in BMP-2, pSmad1/5/8-CT levels were noticeably decreased in shCNT cells compared with shBat3 cells. After 24 h of BMP-2 treatment, pSmad1/5/8-CT was almost undetectable in nuclei of shCNT cells but remained clearly visible in nuclei of shBat3 cells. Quantitation of the signal intensity of nuclear pSmad1/5/8-CT staining in these cultures confirmed a significant increase in pSmad1/5/8-CT in Bat3-depleted cells at 12 or 24 h post BMP but not at earlier time points (Figure 2c). Thus, Bat3 appears to influence the termination of Smad phosphorylation.

We next examined levels of Smad1/5/8-CT phosphorylation in WT and $Bat3^{-/-}$ primary osteoblasts cultured with 100 ng/ml BMP-2 for up to 36 h. As observed in our Bat3-depleted C2C12 cells, levels of pSmad1/5/8-CT were higher in BMP-treated $Bat3^{-/-}$ osteoblasts than in BMP-treated WT osteoblasts (Figure 2d). Moreover, the reintroduction of Bat3–Myc into shBat3 U2OS cells (Supplementary Figure 1C) resulted in lower levels of pSmad1/5/8-CT compared with those in empty vector-transfected shBat3 U2OS cells (Figure 2e). Last, Bat3 depletion in the U2OS also resulted in sustained Smad phosphorylation (increased pSmad1/5/8-CT) upon BMP treatment (Supplementary Figure 1D). Taken together, our data clearly indicate that Bat3 promotes the termination of Smad1/5/8 phosphorylation in response to BMP signaling.

**Bat3 forms a complex with SCP nuclear phosphatases and enhances SCP2–Smad1 interaction.** Our data showed that the induction of BMP target genes was
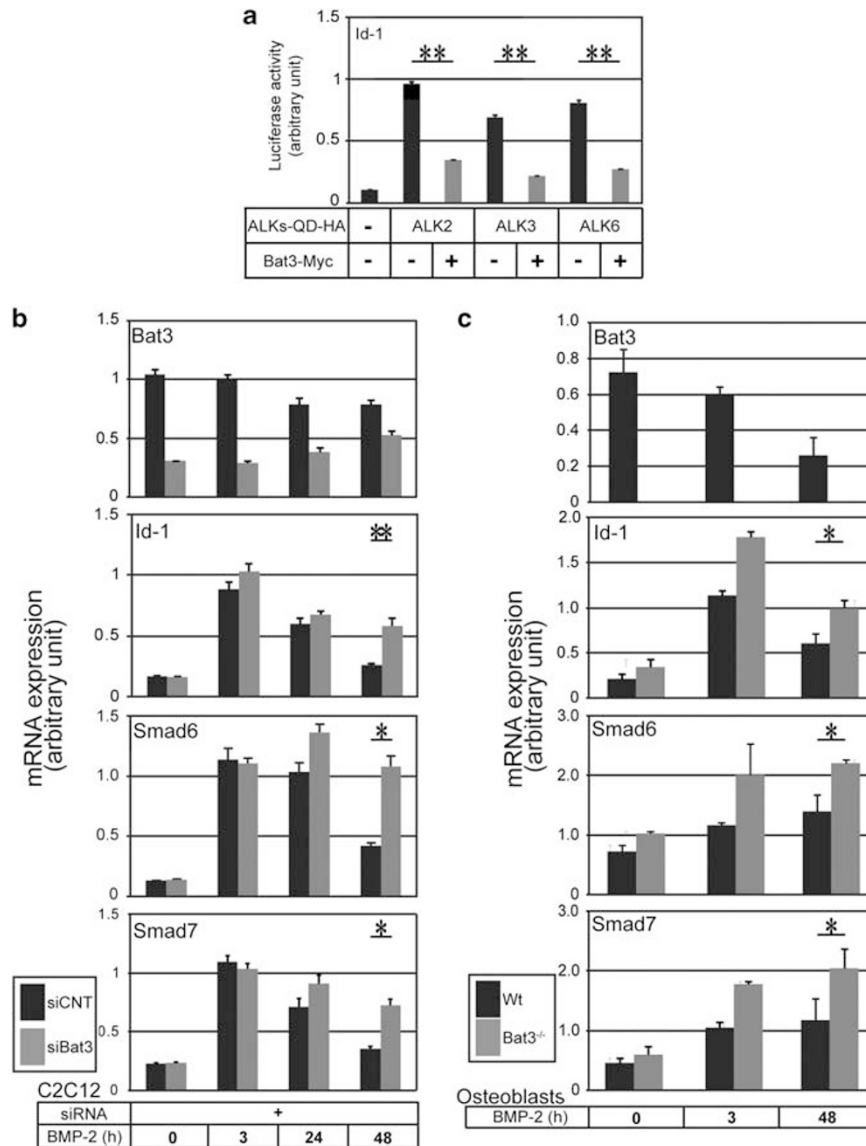
**Figure 1** Loss of Bat3 potentiates BMP signaling. (**a**) Bat3 suppresses Id1 promoter activity. U2OS cells were transiently transfected with an Id1–luc plus the indicated combination of Bat3–Myc and HA-tagged constitutively active (QD) ALK2, 3, and 6 expression vectors. Results are Id1–luc values normalized using Renilla luciferase activity under the control of the cytomegalovirus promoter. (**b**) Prolonged induction of BMP target genes in Bat3-depleted cells. C2C12 cells were transfected with siCNT or siBat3, and treated with 100 ng/ml BMP-2 for the indicated times. Transcript levels of the indicated genes were measured by quantitative RT-PCR and normalized to hypoxanthine phosphoribosyltransferase 1 expression. (**c**) Prolonged induction of BMP target genes in BMP-treated Bat3$^{-/-}$ osteoblasts. Primary osteoblasts from WT and Bat3$^{-/-}$ mice were treated with 100 ng/ml BMP-2 for the indicated times. Transcript levels of the indicated genes were analyzed as in **b**. For **a**, results are the mean ± S.D. of triplicates and are representative of three trials. For **b** and **c**, results are the mean ± S.D. of duplicates and are representative of three trials. \*\*$P < 0.01$ and \*$P < 0.05$

unaffected by Bat3 deficiency at early time points but significantly increased at later time points (Figure 1). In addition, Smad phosphorylation was abnormally prolonged in the absence of Bat3 (Figure 2). We therefore speculated that Bat3's physiological function might be to regulate Smad1/5/8 dephosphorylation. Among the Smad phosphatases, the SCPs, which are nuclear enzymes, have been shown to dephosphorylate Smad1/5/8 at the C terminus and thus attenuate BMP signaling.[26] Accordingly, previous reports have demonstrated that depletion of SCP2 enhances BMP signaling,[26] and that SCPs thus positively regulate TGF-$\beta$ signaling.[8,26] These findings prompted us to explore whether Bat3 was functionally connected to SCPs.

We first tested whether Bat3 could interact with SCP1, 2, or 3 in 293T cells. Co-immunoprecipitation (IP) analysis revealed that Bat3–Myc clearly associated with SCP1 or SCP2 at comparable levels but bound only very weakly to SCP3 (Figure 3a). In addition, recombinant Bat3 and SCP2 proteins interacted (Supplementary Figure 7). We then determined whether Bat3 could interact with the Smurfs and/or I-Smads, which negatively regulate BMP signaling by binding to Smad6 and Smad7, respectively. However, Bat3 did not bind to either Smurf1 or Smurf2, or Smad6 or Smad7 (Figure 3b). Previous work has shown that, although SCP1 and SCP2 show similar enzymatic activities when overexpressed, only SCP2 inactivation inhibits TGF-$\beta$ signaling and enhances BMP
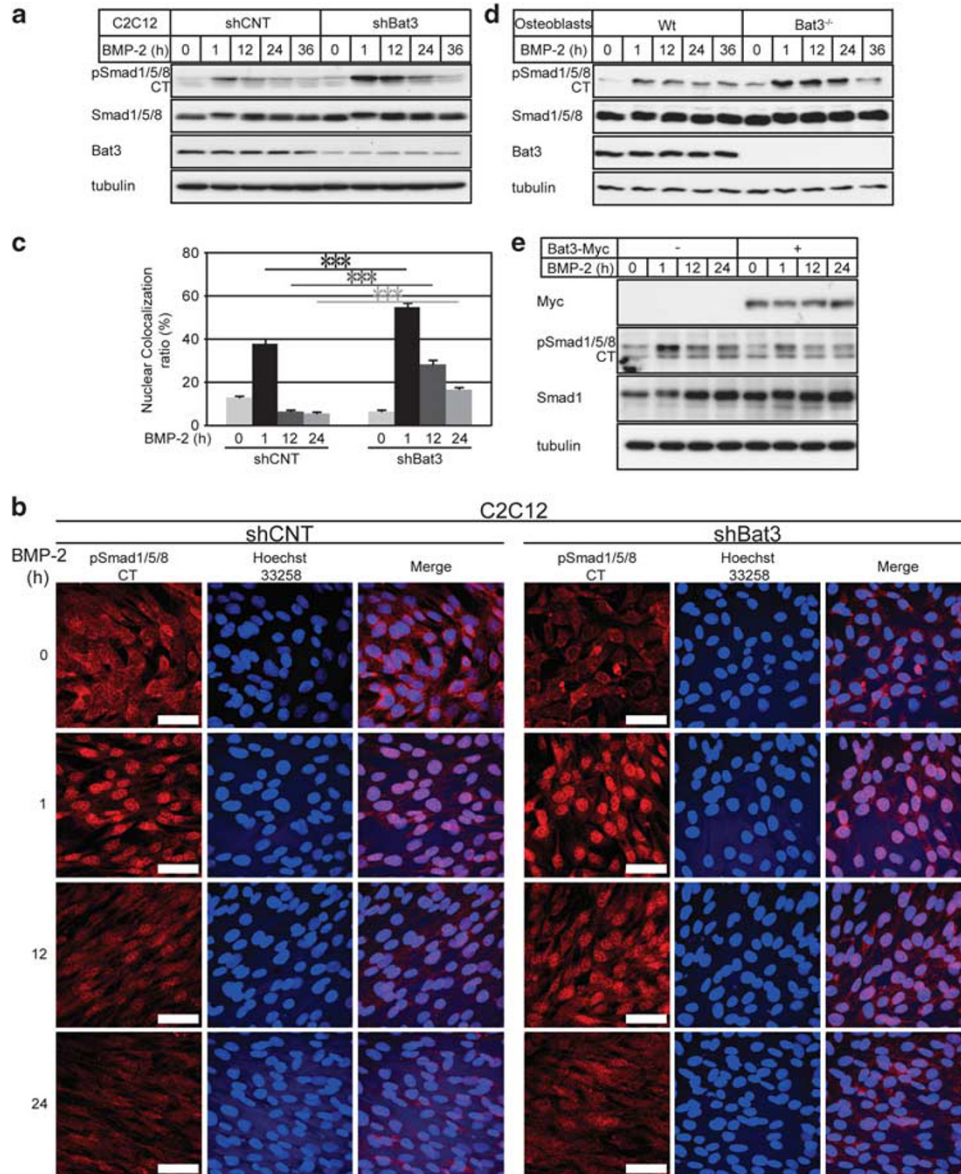
**Figure 2** Bat3 negatively regulates Smad1/5/8 phosphorylation upon BMP treatment. (**a**) Sustained C-terminal phosphorylation of Smad1/5/8 (pSmad1/5/8-CT) in Bat3-depleted cells. C2C12 cells infected with lentivirus expressing shCNT or shBat3 were cultured in the presence of 100 ng/ml BMP-2 for the indicated times. Lysates were immunoblotted to detect the indicated proteins. Tubulin was used as the loading control. (**b**) Nuclear pSmad1/5/8-CT, shCNT, and shBat3 C2C12 cells were treated with 100 ng/ml BMP-2 for the indicated times. Cells were fixed in ice-cold ethanol and stained with anti-phospho Smad1/5/8 Ab, followed by anti-rabbit IgG (red). Nuclei were visualized by Hoechst 33258 (blue). (**c**) Quantitation of nuclear pSmad1/5/8 staining in **b**. FluoView software was used to measure the pixel intensity of pSmad1/5/8 staining that co-localized with Hoechst 33258 staining in each nucleus and shown as percentage. Results are the mean ± S.D. of 30 cells per field for 3 fields. (**d**) Sustained C-terminal phosphorylation of Smad1/5/8 in Bat3$^{-/-}$ osteoblasts. WT and Bat3$^{-/-}$ osteoblasts were treated with 100 ng/ml BMP-2 for the indicated times. Lysates were immunoblotted to detect the indicated proteins as for **a**. (**e**) Reintroduction of Bat3 allows resumption of Smad1/5/8 dephosphorylation in U2OS cells. U2OS cells depleted for Bat3 were transfected with control vector or Bat3–Myc vector. Transfected cells were treated with 25 ng/ml BMP-2 for the indicated times and immunoblotted to detect the indicated proteins as for **d**. Note that the doublet band for pSmads is a cell type-specific phenomenon and was observed only in U2OS cells. For **a–e**, results are representative of three trials. Full-length blots are presented in Supplementary Figure 5

signaling.[8,26] Indeed, we found that SCP2 overexpression reduced Smad1/5/8 phosphorylation induced by ALK6-QD (Supplementary Figure 2). We therefore focused the rest of our study on Bat3's interaction with SCP2.

First, we examined whether Bat3 influenced SCP2's negative regulatory effects on *Id1* promoter activity. We co-transfected U2OS cells with the *Id1*–luc reporter construct plus vectors expressing ALK3-QD and increasing

amounts of SCP2 and Bat3–Myc (Figure 3c). Consistent with previous reports,[8,26] SCP2 suppressed *Id1* promoter activity in a dose-dependent manner in the absence of Bat3. Moreover, consistent with our Figure 1 data, we found that, as the Bat3 level increased, the promoter suppression mediated by SCP2 was enhanced. These findings suggest that a functional interaction occurs between Bat3 and SCP2.
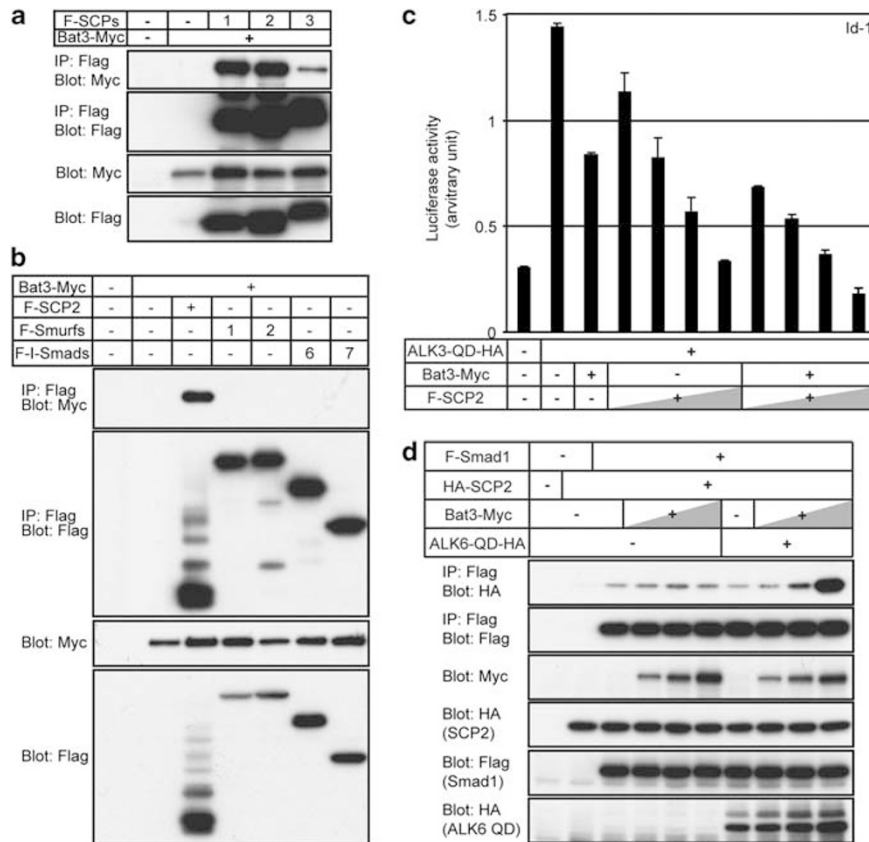
**Figure 3** Bat3 interacts with SCPs and enhances their functions. (**a**) Binding of Bat3 to SCPs. 293T cells were transfected with Bat3–Myc plus empty vector (−) or FLAG-tagged SCP1, SCP2, or -CP3, as indicated. At 24 h post transfection, lysates were immunoprecipitated using anti-FLAG beads and immunoblotted anti-Myc–HRP Ab. (**b**) Bat3 does not interact with Smurfs or I-Smads. 293T cells were transfected with Bat3–Myc plus FLAG–SCP2, FLAG–Smurf1 or –Smurf2, or FLAG–Smad6 or −7, as indicated. Lysates were immunoprecipitated and immunoblotted as for **a**. (**c**) Bat3 enhances SCP2-mediated suppression of Smad transcriptional activity. 293T cells were transfected with the indicated combinations of *Id1*–luc plus tagged ALK3-QD, Bat3, and SCP2 expression vectors. Data were analyzed as for Figure 1a. (**d**) Bat3 enhances SCP2–Smad1 interaction upon activation of BMP signaling. 293T cells were transfected with tagged Smad1, SCP2, and/or ALK6-QD vectors plus increasing amounts of Bat3–Myc. At 24 h post transfection, lysates were immunoprecipitated with anti-FLAG beads and immunoblotted with anti-HA Ab. For **a**–**d**, results are representative of at least three trials. Full-length blots are presented in Supplementary Figure 6

To gain mechanistic insight into this interaction, we tested whether Bat3 influences Smad1–SCP2 binding. We co-transfected 293T cells with tagged vectors expressing Smad1, SCP2, and increasing amounts of Bat3 in the presence or absence of ALK6-QD, and examined Smad1–SCP2 interaction by IP (Figure 3d). Bat3 overexpression did not influence Smad1–SCP2 binding in the absence of ALK6-QD. However, in the presence of ALK6-QD, Smad1–SCP2 interaction was markedly enhanced by Bat3 addition. These data indicate that Bat3 promotes the interaction of SCP2 with the active form of Smad1, and enhances SCP2's subsequent dephosphorylation activity. Thus, our findings constitute additional evidence that Bat3 contributes to the processes terminating BMP signaling.
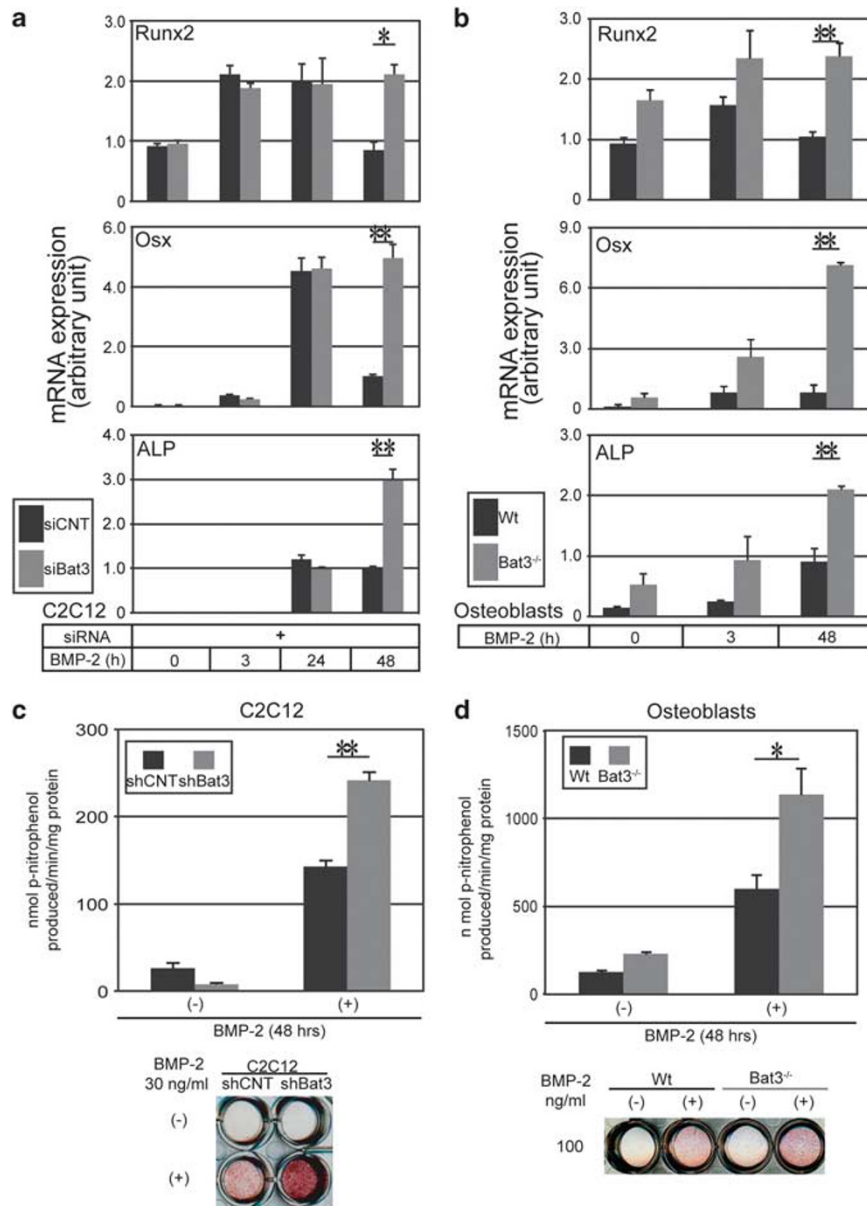
**Bat3 inactivation enhances bone differentiation.** To determine whether Bat3 influences biological responses to BMP, we used bone differentiation as an experimental readout. We cultured C2C12 cells expressing siCNT or siBat3 with 100 ng/ml BMP-2 for 3, 24. or 48 h and examined the transcript levels of the bone differentiation markers *Runx2*, *Osterix*, and *alkaline phosphatase (ALP)*. Induction of

these markers was comparable in control and Bat3-depleted cells up to the 24 h time point (Figure 4a). However, levels of these differentiation markers were significantly higher in the absence of Bat3 after 48 h BMP-2 treatment. Similar results were obtained for BMP-2-treated *Bat3*$^{-/-}$ osteoblasts compared with BMP-treated WT osteoblasts (Figure 4b).

Next, we examined ALP enzymatic activity in Bat3-depleted C2C12 cells (shBat3 cells) and *Bat3*$^{-/-}$ osteoblasts. Consistent with our gene expression analyses, Bat3 inactivation markedly enhanced ALP induction in both cell types (Figures 4c and d). Last, BMP-6-treated *Bat3*$^{-/-}$ mouse embryonic fibroblasts (MEFs) showed the same pattern of elevated pSmad1/5/8, enhanced ALP induction, and increased ALP activity as *Bat3*$^{-/-}$ osteoblasts (Supplementary Figure 3). Taken together, these data point clearly to a role for Bat3 in biological responses to BMP.

## Discussion

It is well established that the level and duration of R-Smad activity has critical effects on TGF-$\beta$-induced transcriptional responses.[27] It is therefore logical that pathways that regulate

**Figure 4** Bat3 inactivation enhances bone differentiation. (**a**) Increased expression of bone differentiation markers in the absence of Bat3. C2C12 cells were transfected with siCNT or siBat3 and treated with 100 ng/ml BMP-2 for the indicated times. Transcript levels of the indicated bone differentiation markers were determined by qPCR. Results were analyzed as for Figure 1b. Results are the mean ± S.D. of duplicates and are representative of three trials. **$P < 0.01$ and *$P < 0.05$. (**b**) Enhanced induction of bone differentiation markers in $Bat3^{-/-}$ osteoblasts. WT and $Bat3^{-/-}$ osteoblasts were treated with BMP-2 for the indicated times. Transcript levels of the indicated markers were analyzed as for **a**. Results are the mean ± S.D. of duplicates and are representative of three trials. **$P < 0.01$ and *$P < 0.05$. (**c** and **d**) Enhanced induction of ALP in the absence of Bat3. (**c**) shCNT and shBat3 C2C12 cells were treated with 30 ng/ml BMP-2 for 48 h, and (**d**) WT and $Bat3^{-/-}$ osteoblasts were treated with 100 ng/ml BMP-2 for 48 h. In both cases, levels of ALP activity were measured *in situ* using a plate staining assay with *p*-nitrophenyl phosphate as the substrate. Top panels: absorbance in extracts of plated cells was normalized to protein concentration. All measurements are relative to time zero (set to one). Bottom panels: representative images of stained plates showing ALP activity. For **c**, results are the mean ± S.D. of duplicates and are representative of three trials. For **d**, results are the mean ± S.D. of triplicates and are representative of two trials. **$P < 0.01$

the dephosphorylation inactivating R-Smads would have a significant impact on TGF-$\beta$ and BMP signaling. Although multiple Smad phosphatases have been identified,[28] it has been unclear how the activity and expression of these phosphatases are regulated. In this study, we have shown that Bat3 promotes Smad1/5/8 dephosphorylation and thereby influences BMP signaling. In addition, we have started to unravel the molecular mechanisms underlying this regulation.

The regulation of R-Smad dephosphorylation has been difficult to dissect, partly because of the diverse and dynamic functions of these phosphatases, and partly because of our poor understanding of the tissue-specific mechanisms that control these enzymes.[29] Among the known Smad phosphatases, the SCPs have been reported to differentially regulate Smad2/3 and Smad1/5/8.[7,8,26] SCP1 and 2 clearly dephosphorylate the linker regions of Smad2 and 3, thereby

enhancing TGF-$\beta$ signaling. However, controversy exists over whether SCP-mediated dephosphorylation of sites within the linker and C-terminal regions of Smad1 can inactivate this molecule, thereby suppressing BMP signaling.[7,8,26] Our study has partially resolved this issue by demonstrating that SCP2 can indeed dephosphorylate the C-terminal phosphorylation sites in Smad1 and Smad5, while showing weaker activity for Smad8 (Supplementary Figure 2). It is currently unknown whether SCPs require additional factors and/or modifications to initiate Smad1 dephosphorylation, or whether SCP-mediated Smad1 dephosphorylation is tissue or species specific. Nevertheless, our data indicate that Smad1–SCP2 interaction is enhanced by Bat3, and that this series of events regulates BMP signaling (Figure 3).

Bat3 has been reported to act as a regulator of molecular chaperone proteins,[30] and also contains a ubiquitin-like (UBL) domain. Therefore, like other UBL-containing proteins,[31] Bat3 may suppress or enhance protein stability, protein–protein interactions, or both. Although Bat3 target proteins have yet to be fully delineated, our biochemical analyses indicate that SCP2 is a Bat3-interacting protein. Interestingly, Bat3 enhances Smad1–SCP2 interaction only in the presence of constitutively active ALK6 (Figure 3). It has been previously shown that ALK5–Bat3 interaction accelerates the translocation of Bat3 into the nucleus.[22] However, in the context of BMP signaling, we were unable to detect any interaction between Bat3 and ALK2, 3, or 6 (Supplementary Figure 4). In addition, Bat3 is located predominantly in the nucleus in the cell lines used in our study, obscuring any increase in levels of total Bat3 protein or nuclear Bat3 protein that might have been induced by BMP treatment (Figure 2, Supplementary Figure 1 and data not shown). Finally, although our data strongly suggest that Bat3 enhances the interaction between SCP and phosphorylated Smad1, it remains to be elucidated whether additional post-translational modifications (e.g., ubiquitination or acetylation) of Smad1, SCP2, and/or Bat3 are required for physiological regulation of BMP signaling.

In their detailed analyses of the developmental defects of Bat3-deficient mice, Desmots et al.[15] reported that these mutants showed impaired branching of the terminal bronchiolar alveoli in the lung as well as abnormal renal branching in the kidney, two processes for which BMP signaling is known to be crucial.[32–34] These in vivo findings raised the possibility that dysregulated BMP signaling might be responsible for the defects in their Bat3-deficient mice. Our demonstration in cell lines that Bat3 inactivation sustained BMP signaling and enhances osteoblast differentiation support a role for Bat3 in development. However, further investigation of tissue-specific Bat3 knockout mice will be required to confirm any such in vivo functions for Bat3.

In conclusion, our work demonstrates that Bat3 positively regulates dephosphorylation of Smad1/5/8 and thus functions as a negative regulator of BMP signaling. As BMPs enhance bone generation, modification of the BMP–Bat3 signaling may improve efficacy of bone replacement and implant. In addition, because dysregulation of the TGF-$\beta$ and BMP signaling pathways has been observed in numerous human disorders, including cancer,[32,35,36] it would be interesting to determine whether mutations of Bat3 are associated with disease progression.

## Materials and Methods

**Primary cells from mice.** Bat3$^{-/-}$ mice have been previously described.[17] Primary osteoblasts were isolated from individual calvaria of newborn (P3 or P4) WT and Bat3$^{-/-}$ mice as previously described.[37] Bat3-deficient and WT MEFs were prepared from E13.5 embryos using a standard procedure.[38] Primary osteoblasts were maintained in $\alpha$-MEM medium, and MEFs were maintained in Dulbecco's modified Eagle's medium (DMEM; both from Invitrogen, Burlington, ON, Canada). Media were supplemented with 10% fetal bovine serum (FBS; Wisent, ST-Bruno, QC, Canada), penicillin (100 U/ml), and streptomycin (100 $\mu$g/ml). Cells were cultured at 37°C in a humidified atmosphere containing 5% $CO_2$.

**Cell lines.** U2OS cells, C2C12 cells, and 293T cells were originally obtained from the American Type Culture Collection (Manassas, VA, USA). U2OS cells were maintained in McCoy 5A medium, and 293T and C2C12 cells were maintained in DMEM (both from Invitrogen). Media were supplemented with 10% FBS (Wisent), penicillin (100 U/ml), and streptomycin (100 $\mu$g/ml). Cells were cultured at 37°C in a humidified atmosphere containing 5% $CO_2$.

**BMP stimulation.** Cells were seeded at a density of $1.0 \times 10^5$ cells per well on collagen-I-coated 12-well plates and cultured for 24 h. The culture medium was then replaced with 1.0% FBS-containing medium for 4 h before the addition of 25–100 ng/ml (final concentration) of recombinant BMP-2 or BMP-6 (R&D Systems, Minneapolis, MN, USA) as previously described.[33] After BMP stimulation, cells were harvested for biochemical or histochemical analyses as described below.

**DNA transfection.** The constructs expressing Bat3, Smads, or constitutively active forms of BMP type I receptors (ALKs) have been described previously.[17,24] Cells were transfected with plasmids using FuGENE6 transfection reagent (Roche Diagnostics, Mississauga, ON, Canada) or Lipofectamine 2000 transfection reagent (Invitrogen) according to the manufacturer's recommendations.

**siRNA transfection.** Synthetic siRNA oligo duplexes for mouse and human Bat3 were purchased from Dharmacon Inc. (Lafayette, CO, USA). The human Bat3 siRNA oligo-duplex sequence was as previously described,[17] and the mouse Bat3 siRNA oligo-duplex sequence was 5′-GAUCUGCGCUGCAAUCUAG-3′ or 5′-GCACGUGGUUCGGCCUAUG-3′. For siRNA-mediated gene silencing, cells were transfected with siRNA oligo duplexes (final concentration, 40 nM) using Hiperfect (Qiagen, Toronto, ON, Canada). All control samples were transfected with control siRNA oligo duplex (Dharmacon Inc.). At 48 h post transfection, the transfected cells were cultured in 1.0% FBS-containing medium for 4 h before BMP stimulation as above.

**Lentiviral shRNA transfection.** Target sequences of shRNA were chosen from siRNA oligos based on their knockdown efficiency. Annealed oligos were subcloned into pLKO.1 (Addgene, Cambridge, MA, USA).[39] For lentivirus production, $2.5 \times 10^6$ HEK-293T cells were plated in a 6-cm tissue culture dish and transfected with shRNA plasmids using FuGENE6 (Roche Diagnostics) according to the manufacturer's protocol. After 24 h incubation at 37°C in 5% $CO_2$, the culture medium was replaced with 5 ml fresh DMEM containing 10% FBS and antibiotics. Culture supernatants were harvested after 24 h, filtered through a 0.45 $\mu$m filter, and used immediately for experiments, or aliquoted and stored in −80°C freezer for subsequent use.

**ALP analyses.** Histochemical analysis was performed using the ALP staining kit (no. 85L-3R; Sigma, Oakville, ON, Canada) according to the manufacturer's protocol. Quantitative analysis of ALP activity was performed as previously described,[40] using Sigma Fast p-nitrophenyl phosphate tablet sets (Sigma). The data were normalized to protein concentration measured by the BCA Protein Assay Reagent Kit (Pierce, Nepean, ON, Canada) using bovine serum albumin as the standard. All measurements were relative to time zero, which was set to one.

**Luciferase assay.** The transcriptional activation induced by constitutively active ALK (ALK-QD) was measured using Id1–luc reporter constructs.[41] U2OS cells were seeded in 12-well plates (BD Falcon, Mississauga, ON, Canada) and transiently transfected with the appropriate combinations of reporter construct and expression plasmids. At 24 h post transfection, cell lysates were prepared, and luciferase activities were measured by the Dual-Luciferase reporter system (Promega, Madison, WI, USA) using a luminometer (Turner Biosystems Luminometer, Promega). Values were normalized using Renilla luciferase activity under the control of the cytomegalovirus promoter.

**IP and immunoblotting.** For IP, cells were harvested in Nonidet P-40 lysis buffer consisting of 150 mM NaCl, 50 mM Tris-HCl (pH 7.4), 1% Nonidet P-40, 1 mM phenylmethylsulfonyl fluoride (PMSF), and protease inhibitor cocktail (Roche Diagnostics). Lysates were centrifuged and supernatants were incubated with the appropriate antibodies at 4°C for 16 h with rotation. For immune complex isolation, lysate–Ab mixtures were incubated for an additional 0.5–1 h with protein A/G agarose beads (Santa Cruz Biotechnology, Santa Cruz, CA, USA) before fractionation. Immune complexes or immunoprecipitates were fractionated by SDS-PAGE and subjected to immunoblotting using standard procedures.

For protein analysis, samples were prepared in RIPA lysis buffer consisting of 1% Nonidet P-40, 50 mM Tris-HCl (pH 7.4), 150 mM NaCl, 1 mM EDTA (pH 8.0), 0.5% sodium deoxycholate, 0.1% SDS, 2 mM NaF, protease inhibitor cocktail (Roche Diagnostics), and 1 mM PMSF.

Antibodies recognizing the following proteins were used: Smad1/5/8 (N-18; Santa Cruz Biotechnology), Smad1 (Invitrogen), phospho-Smad1/5/8 (Cell Signaling, Pickering, ON, Canada), Flag (M2; Sigma), Myc (Sigma), $\alpha$-tubulin (DM1A; Sigma), $\beta$-actin (Sigma), and HA (Roche Diagnostics). Anti-Bat3 Ab has been previously described.[17]

**Quantitative real-time reverse transcription PCR.** Total RNA was extracted from C2C12 cells or primary osteoblasts using the RNeasy plus Mini Kit (Qiagen). cDNA was synthesized using SuperScript III reverse transcriptase (Invitrogen), followed by PCR specific for target genes (primer sequences are listed in Supplementary Table S1 in Supplementary Information). Real-time PCR was performed using Power SYBR Green PCR Master Mix (Applied Biosystems, Streetsville, ON, Canada), and data were collected using the ABI Prism 7900HT Fast Real-time PCR system (Applied Biosystems). The specificity of the detected signals was confirmed by observation of a dissociation curve containing a single peak. Data were normalized to expression levels of hypoxanthine phosphoribosyltransferase 1.

**Immunofluorescent microscopy.** Cells were fixed in ice-cold 100% ethanol at 0, 1, 12, and 24 h post BMP treatment for 15 min at −20°C and blocked in CAS-BLOCK (Invitrogen) for 10 min at room temperature. Slides were incubated with rabbit anti-phospho-Smad1/5/8 (Cell Signaling) as the primary Ab, followed by Alexa Fluor 594 goat anti-rabbit IgG (Invitrogen). Hoechst 33258 (Invitrogen) was used to stain DNA. Images were acquired on an Olympus (Richmond Hill, ON, Canada) IX81 and FluoView FL1000 confocal microscope using a × 63/1.2 NA water immersion objective. Hoechst 33258 and Alexa 594 signals were imaged sequentially using 351- and 543-nm laser excitation and the appropriate band-pass emission filters.

**Production of recombinant proteins.** Escherichia coli (BL21 (DE3)) transformed with GST or GST–SCP2 were lysed with RIPA buffer (50 mM Tris-HCl, pH 8.0, 150 mM NaCl, 1 mM EDTA, 1 mM DTT, 1 mM PMSF, protease inhibitor cocktail (Roche Diagnostics), and 1% Triton-X 100 for 30 min on ice and sonicated three times for 30 s on ice. Cell lysates were cleared by centrifugation at 4150 × g for 60 min at 4°C. Lysates were incubated with 100 μl of 50% slurry of glutathione Sepharose 4 Fast Flow (GE Healthcare Life Sciences, Baie d'Urfe, QC, Canada) for 1 or 2 h at 4°C with end-over-end rotation. The glutathione beads were then collected by centrifugation at 2500 × g for 2 min at 4°C and washed five times with ice-cold PBS. Overexpression of 6 × His-tagged recombinant protein Bat3 was purified by Ni-NTA column (Qiagen) according to the manufacturer's instructions. Each sample was confirmed by GelCode Blue Stain Reagent (Thermo Scientific, Nepean, ON, Canada).

**GST pull down assay.** Purified Bat3–His lysates (500 μl) were incubated with 100 μl of a 50% slurry of GST or GST–SCP2 binding glutathione Sepharose 4 Fast Flow for 4 h at 4°C with rotation. The bound proteins were then released by boiling for 3 min at 98°C in 1 × SDS-PAGE sample buffer for subsequent immunoblot analysis. Ab used was anti-GST Ab (GE Healthcare Life Sciences).

**Conflict of Interest**

The authors declare no conflict of interest.

**Author contributions**

KG and HO designed the research; KG, KIT, and JI performed the experiments; KG and HO analyzed the data; and HO wrote the paper with contributions from the listed coauthors.

1. Feng XH, Derynck R. Specificity and versatility in tgf-beta signaling through Smads. Annu Rev Cell Dev Biol 2005; 21: 659–693.
2. Moustakas A, Heldin CH. The regulation of TGFbeta signal transduction. Development 2009; 136: 3699–3714.
3. Watabe T, Miyazono K. Roles of TGF-beta family signaling in stem cell renewal and differentiation. Cell Res 2009; 19: 103–115.
4. Lin X, Duan X, Liang YY, Su Y, Wrighton KH, Long J et al. PPM1A functions as a Smad phosphatase to terminate TGFbeta signaling. Cell 2006; 125: 915–928.
5. Duan X, Liang YY, Feng XH, Lin X. Protein serine/threonine phosphatase PPM1A dephosphorylates Smad1 in the bone morphogenetic protein signaling pathway. J Biol Chem 2006; 281: 36526–36532.
6. Chen HB, Shen J, Ip YT, Xu L. Identification of phosphatases for Smad in the BMP/DPP pathway. Genes Dev 2006; 20: 648–653.
7. Knockaert M, Sapkota G, Alarcon C, Massague J, Brivanlou AH. Unique players in the BMP pathway: small C-terminal domain phosphatases dephosphorylate Smad1 to attenuate BMP signaling. Proc Natl Acad Sci USA 2006; 103: 11940–11945.
8. Wrighton KH, Willis D, Long J, Liu F, Lin X, Feng XH. Small C-terminal domain phosphatases dephosphorylate the regulatory linker regions of Smad2 and Smad3 to enhance transforming growth factor-beta signaling. J Biol Chem 2006; 281: 38365–38375.
9. Thress K, Henzel W, Shillinglaw W, Kornbluth S. Scythe: a novel reaper-binding apoptotic regulator. EMBO J 1998; 17: 6135–6143.
10. Banerji J, Sands J, Strominger JL, Spies T. A gene pair from the human major histocompatibility complex encodes large proline-rich proteins with multiple repeated motifs and a single ubiquitin-like domain. Proc Natl Acad Sci USA 1990; 87: 2374–2378.
11. Pogge von Strandmann E, Simhadri VR, von Tresckow B, Sasse S, Reiners KS, Hansen HP et al. Human leukocyte antigen-B-associated transcript 3 is released from tumor cells and engages the NKp30 receptor on natural killer cells. Immunity 2007; 27: 965–974.
12. Nguyen P, Bar-Sela G, Sun L, Bisht KS, Cui H, Kohn E et al. BAT3 and SET1A form a complex with CTCFL/BORIS to modulate H3K4 histone dimethylation and gene expression. Mol Cell Biol 2008; 28: 6720–6729.
13. Thress K, Kornbluth S, Smith JJ. Mitochondria at the crossroad of apoptotic cell death. J Bioenerg Biomembr 1999; 31: 321–326.
14. Thress K, Evans EK, Kornbluth S. Reaper-induced dissociation of a Scythe-sequestered cytochrome c-releasing activity. EMBO J 1999; 18: 5486–5493.
15. Desmots F, Russell HR, Lee Y, Boyd K, McKinnon PJ. The reaper-binding protein scythe modulates apoptosis and proliferation during mammalian development. Mol Cell Biol 2005; 25: 10329–10337.
16. Adams JM, Harris AW, Pinkert CA, Corcoran LM, Alexander WS, Cory S et al. The c-myc oncogene driven by immunoglobulin enhancers induces lymphoid malignancy in transgenic mice. Nature 1985; 318: 533–538.
17. Sasaki T, Gan EC, Wakeham A, Kornbluth S, Mak TW, Okada H. HLA-B-associated transcript 3 (Bat3)/Scythe is essential for p300-mediated acetylation of p53. Genes Dev 2007; 21: 848–861.
18. Mariappan M, Li X, Stefanovic S, Sharma A, Mateja A, Keenan RJ et al. A ribosome-associating factor chaperones tail-anchored membrane proteins. Nature 2010; 466: 1120–1124.
19. Leznicki P, Clancy A, Schwappach B, High S. Bat3 promotes the membrane integration of tail-anchored proteins. J Cell Sci 2010; 123: 2170–2178.
20. Hessa T, Sharma A, Mariappan M, Eshleman HD, Gutierrez E, Hegde RS. Protein targeting and degradation are coupled for elimination of mislocalized proteins. Nature 2011; 475: 394–397.
21. Minami R, Hayakawa A, Kagawa H, Yanagi Y, Yokosawa H, Kawahara H. BAG-6 is essential for selective elimination of defective proteasomal substrates. J Cell Biol 2010; 190: 637–650.
22. Kwak JH, Kim SI, Kim JK, Choi ME. BAT3 interacts with transforming growth factor-beta (TGF-beta) receptors and enhances TGF-beta1-induced type I collagen expression in mesangial cells. J Biol Chem 2008; 283: 19816–19825.
23. de Jong DS, Vaes BL, Dechering KJ, Feijen A, Hendriks JM, Wehrens R et al. Identification of novel regulators associated with early-phase osteoblast differentiation. J Bone Miner Res 2004; 19: 947–958.
24. Goto K, Kamiya Y, Imamura T, Miyazono K, Miyazawa K. Selective inhibitory effects of Smad6 on bone morphogenetic protein type I receptors. J Biol Chem 2007; 282: 20603–20611.
25. Wrighton KH, Lin X, Feng X-H. Phospho-control of TGF-beta superfamily signaling. Cell Res 2009; 19: 8–20.
26. Sapkota G, Knockaert M, Alarcón C, Montalvo E, Brivanlou AH, Massagué J. Dephosphorylation of the linker regions of Smad1 and Smad2/3 by small C-terminal domain phosphatases has distinct outcomes for bone morphogenetic protein and transforming growth factor-beta pathways. J Biol Chem 2006; 281: 40412–40419.

27. Nicolas FJ, Hill CS. Attenuation of the TGF-beta-Smad signaling pathway in pancreatic tumor cells confers resistance to TGF-beta-induced growth arrest. *Oncogene* 2003; **22**: 3698–3711.

28. Liu T, Feng XH. Regulation of TGF-beta signalling by protein phosphatases. *Biochem J* 2010; **430**: 191–198.

29. Derynck R, Miyazono Ko. *The TGF-[beta] Family.* Cold Spring Harbor Laboratory Press: Cold Spring Harbor, New York, USA, 2008.

30. Thress K, Song J, Morimoto RI, Kornbluth S. Reversible inhibition of Hsp70 chaperone function by Scythe and Reaper. *EMBO J* 2001; **20**: 1033–1041.

31. Hochstrasser M. Origin and function of ubiquitin-like proteins. *Nature* 2009; **458**: 422–429.

32. Ikushima H, Miyazono K. TGFbeta signalling: a complex web in cancer progression. *Nat Rev Cancer* 2010; **10**: 415–424.

33. Que J, Choi M, Ziel JW, Klingensmith J, Hogan BL. Morphogenesis of the trachea and esophagus: current players and new roles for noggin and Bmps. *Differentiation* 2006; **74**: 422–437.

34. Bachiller D, Klingensmith J, Kemp C, Belo JA, Anderson RM, May SR *et al.* The organizer factors Chordin and Noggin are required for mouse forebrain development. *Nature* 2000; **403**: 658–661.

35. Meulmeester E, Ten Dijke P. The dynamic roles of TGF-beta in cancer. *J Pathol* 2011; **223**: 205–218.

36. Massague J. TGFbeta in cancer. *Cell* 2008; **134**: 215–230.

37. Suh WK, Wang SX, Jheon AH, Moreno L, Yoshinaga SK, Ganss B *et al.* The immune regulatory protein B7-H3 promotes osteoblast differentiation and bone mineralization. *Proc Natl Acad Sci USA* 2004; **101**: 12969–12973.

38. Okada H, Suh WK, Jin J, Woo M, Du C, Elia A *et al.* Generation and characterization of Smac/DIABLO-deficient mice. *Mol Cell Biol* 2002; **22**: 3509–3517.

39. Moffat J, Grueneberg DA, Yang X, Kim SY, Kloepfer AM, Hinkle G *et al.* A lentiviral RNAi library for human and mouse genes applied to an arrayed viral high-content screen. *Cell* 2006; **124**: 1283–1298.

40. Maeda S, Hayashi M, Komiya S, Imamura T, Miyazono K. Endogenous TGF-beta signaling suppresses maturation of osteoblastic mesenchymal cells. *EMBO J* 2004; **23**: 552–563.

41. Kahata K, Hayashi M, Asaka M, Hellman U, Kitagawa H, Yanagisawa J *et al.* Regulation of transforming growth factor-beta and bone morphogenetic protein signalling by transcriptional coactivator GCN5. *Genes Cells* 2004; **9**: 143–151.

Supplementary Information accompanies the paper on Cell Death and Disease website (http://www.nature.com/cddis)